Neuroscience 152 (2008) 990–1005

CLONING AND MOLECULAR CHARACTERIZATION OF THE ORPHAN CARRIER PROTEIN Slc10a4: EXPRESSION IN CHOLINERGIC NEURONS OF THE RAT CENTRAL NERVOUS SYSTEM

J. GEYER,[a1]* C. F. FERNANDES,[a1] B. DÖRING,[a] S. BURGER,[a] J. R. GODOY,[a] S. RAFALZIK,[b] T. HÜBSCHLE,[b] R. GERSTBERGER[b] AND E. PETZINGER[a]

[a]*Institute of Pharmacology and Toxicology, Justus Liebig University of Giessen, Frankfurter Str. 107, 35392 Giessen, Germany*

[b]*Institute of Veterinary Physiology, Justus Liebig University of Giessen, Frankfurter Str. 100, 35392 Giessen, Germany*

Abstract—We report on the cloning and molecular characterization of the rat carrier Slc10a4 and its cellular localization in the CNS by immunohistochemistry. Slc10a4 is the rat counterpart of the human orphan carrier SLC10A4, which was recently reported to be highly expressed in brain and placenta. Both carriers belong to the solute carrier family SLC10, formerly named the "sodium/bile acid cotransporter family." So SLC10A4/Slc10a4 has a phylogenetic relationship to the Na^+/taurocholate cotransporting polypeptide Ntcp (Slc10a1) and the apical sodium-dependent bile acid transporter Asbt (Slc10a2). The rat Slc10a4 protein consists of 437 amino acids and exhibits a seven transmembrane domain topology with N_{exo}/C_{cyt} *trans*-orientation of the N- and C-terminal ends. Expression of the Slc10a4 protein was detected in motor regions of the spinal cord and rhombencephalon, as well as in mesopontine cholinergic neurons, the medial habenula, cholinergic areas of the forebrain, and the gut myenteric plexus. Co-localization studies with the cholinergic marker proteins choline acetyltransferase (ChAT), vesicular acetylcholine transporter (VAChT), and high-affinity choline transporter (CHT1) demonstrated expression of Slc10a4 in cholinergic neurons. Despite its close phylogenetic relationship to Ntcp, Slc10a4 showed no transport activity for the Ntcp substrates taurocholate, estrone-3-sulfate, dehydroepiandrosterone sulfate, and pregnenolone sulfate when expressed in HEK293 cells or *Xenopus laevis* oocytes. Slc10a4 also did not transport choline, which is a substrate of CHT1. Although the functional properties of Slc10a4 could not be elucidated in this study, Slc10a4 is regarded as a new marker protein for cholinergic neurons in the rat CNS.

Key words: Slc10a4, bile acid transport, ChAT, VAChT, CHT1, cholinergic system.

In the CNS, interneuronal signal transduction via synapses often involves the retrieval of the neurotransmitter (NT) from the synaptic cleft and its restorage into presynaptic vesicles (Masson et al., 1999; Gether et al., 2006). NT reuptake across the presynaptic membrane in general represents a sodium-dependent and partially chloride-dependent process mediated by transporter proteins of the solute carrier families SLC1 and SLC6 (e.g. the transporters for dopamine, 5-HT, norepinephrine, glutamate, GABA, or glycine) (Chen et al., 2004; Kanai and Hediger, 2003). The high-affinity sodium-dependent choline transporter CHT1 (SLC5A7) also belongs to this class of carrier proteins (Apparsundaram et al., 2000; Okuda et al., 2000; Okuda and Haga, 2000). The coupling of substrate transport to ion gradients allows uphill accumulation of NT molecules against their electrochemical gradient and embodies a general principle also for other SLC families (Hediger et al., 2004).

One of these SLC families is the solute carrier family 10 (SLC10) of which human SLC10A4 represents a recently discovered member with high mRNA expression in brain, placenta, and pancreas (Splinter et al., 2006). The discovery of high SLC10A4 expression, especially in the brain, was unexpected, because the two classic representatives of this carrier family are bile acid transporters of hepatic and intestinal origin. These are 1) the Na^+/taurocholate cotransporting polypeptide Ntcp (Slc10a1) (Hagenbuch et al., 1990, 1991), which is exclusively localized at the sinusoidal membrane of hepatocytes (Ananthanarayanan et al., 1994; Stieger et al., 1994), and 2) the apical sodium-dependent bile acid transporter Asbt (Slc10a2), which is expressed and translocated to the apical brush border membrane of enterocytes (Wong et al., 1994; Shneider et al., 1995). Both carrier proteins promote the enterohepatic circulation of bile acids and have important roles in liver physiology (Meier and Stieger, 2002; Trauner and Boyer, 2003; Alrefai and Gill, 2007). Additional members of the SLC10 carrier family have recently been identified, including the sodium-dependent organic anion transporter Soat (Slc10a6), which transports sulfoconjugated steroid hormones and sulfoconjugated bile acids (Geyer et al., 2004a, 2007), and the orphan carrier proteins Slc10a5, and Slc10a7 (Fernandes et al., 2007; Godoy et al., 2007), but none of them showed noticeable expression in the brain.

In the present study, we report on the cloning and molecular characterization of the rat Slc10a4 protein and its cellular distribution in the rat CNS and enteric nervous system. Here, the Slc10a4 protein proved to be expressed

[1] These authors contributed equally to this work.

*Corresponding author. Tel: +49-641-9938404; fax: +49-641-9938419.
E-mail address: Joachim.M.Geyer@vetmed.uni-giessen.de (J. Geyer).

Abbreviations: Asbt, apical sodium-dependent bile acid transporter; BSA, bovine serum albumin; ChAT, choline acetyltransferase; CHT1, high-affinity choline transporter; CMV, cytomegalovirus; C_T, threshold cycle; DHEAS, dehydroepiandrosterone sulfate; HA, hemagglutinin; HEK293, human embryonic kidney 293 cells; IgG, immunoglobulin G; NT, neurotransmitter; Ntcp, Na^+/taurocholate cotransporting polypeptide; PB, phosphate buffer; PBS, phosphate-buffered saline; PREGS, pregnenolone sulfate; SLC10, solute carrier family 10; SN, substantia nigra; Soat, sodium-dependent organic anion transporter; TMD, transmembrane domain; VAChT, vesicular acetylcholine transporter.

0306-4522/08$32.00+0.00 © 2008 IBRO. Published by Elsevier Ltd. All rights reserved.
doi:10.1016/j.neuroscience.2008.01.049

in cholinergic neurons and co-localized with the cholinergic marker proteins CHT1, vesicular acetylcholine transporter (VAChT), and choline acetyltransferase (ChAT).

EXPERIMENTAL PROCEDURES

Radiochemicals

[1,2,6,7-^{3}H(N)]Dehydroepiandrosterone sulfate (DHEAS) (60 Ci/mmol), [6,7-^{3}H(N)]estrone-3-sulfate (57.3 Ci/mmol), and [^{3}H]taurocholate (3.5 Ci/mmol) were purchased from PerkinElmer (Boston, MA, USA). [7-^{3}H(N)]Pregnenolone-3-sulfate (20 Ci/mmol) and [^{3}H]choline chloride (85 Ci/mmol) were obtained from American Radiolabeled Chemicals (St. Louis, MO, USA).

Animals

Animal care, breeding, and experimental procedures were conducted according to the guidelines on the ethical use of animals approved by the Hessian Ethical Committee. Attempts were made to minimize the number of animals used and their suffering. Ten male Wistar rats (180–250 g) bred at the Dept. of Veterinary Physiology were used in this study. The rats were housed individually in polycarbonate type IV cages with *ad libitum* access to standard laboratory chow and water. Room temperature was controlled at 24±1 °C and relative humidity at 60%. Lights were on from 7:00 AM to 7:00 PM. Mature female *Xenopus laevis* frogs were purchased from H. Kähler (Hamburg, Germany) and kept under standard conditions as described (Colman, 1984).

Cloning of rat Slc10a4

For the cloning of rat Slc10a4, we used an RT-PCR based approach, starting from a hitherto uncharacterized cDNA sequence (GenBank accession number XM_579196) that was predicted by automated computational analysis from the rat genome and which showed 82% sequence identity to a human cDNA sequence deposited in 2001 (GenBank accession number BC012048), later annotated as SLC10A4. The following oligonucleotide primers including *Sac*I/*Xba*I restriction sites were derived from this sequence and were employed for PCR amplification: 5′-cga cga gct cat gga cgg cct gga caa cac cac-3′ forward and 5′-ctt cta gat cag agg gaa gtc tgg gtg gtt tc-3′ reverse. RT-PCR was carried out starting from 1 μg rat adrenal gland polyA$^+$RNA with the Expand High Fidelity PCR system (Roche, Mannheim, Germany). The amplicon was gel purified and digested for 90 min at 37 °C with *Xba*I and *Sac*I. The sticky ended cDNA fragment was directionally ligated downstream from the T3 promoter into pBluescript (Stratagene, Heidelberg, Germany) predigested with the respective restriction enzymes (*Sac*I and *Xba*I). Three different clones were sequenced for both strands (SeqLab Laboratories, Göttingen, Germany), and the rat Slc10a4 cDNA sequence was deposited into the GenBank database with accession number AY825923 (release date December 6th, 2004).

Real-time quantitative PCR analysis

Relative SLC10A4/Slc10a4 expression analysis was performed with ABI PRISM 7300 technology (Applied Biosystems, Darmstadt, Germany) using cDNA panels and RNA samples from commercial suppliers (Clontech and BioCat, Heidelberg, Germany). PCR amplification was achieved with the TaqMan Gene Expression Assays, Hs00293728_m1 for human SLC10A4 and Hs99999903_m1 for human β-actin. The assays Mm00557788_m1 and Rn02350050_m1 were used for the quantification of mouse and rat Slc10a4 mRNA expression, respectively. Additionally, the assays Mm00607939_s1 and Rn00667869_m1 were used for quantification of mouse and rat β-actin, respectively. The expression data of β-actin in each tissue was used as an endogenous control. For each tissue, quadruplicate determinations were performed in a 96-well optical plate for each target (SLC10A4/Slc10a4 and β-actin) using 5 μl cDNA, 1.25 μl TaqMan Gene Expression Assay, 12.5 μl TaqMan Universal PCR Master Mix, and 6.25 μl water in each 25 μl reaction. The plates were heated for 10 min at 95 °C, and 45 cycles of 15 s at 95 °C and 60 s at 60 °C were applied. Relative SLC10A4/Slc10a4 expression (ΔC_T) was calculated by subtracting the signal threshold cycle (C_T) of β-actin from the C_T value of SLC10A4/Slc10a4. Then $\Delta\Delta C_T$ values were calculated by subtracting the ΔC_T value of the organ with the lowest expression of each panel from the ΔC_T value of each individual tissue and transformed by the equation $2^{-\Delta\Delta CT}$.

Insertion of the FLAG epitope

In order to evaluate whether the Slc10a4 protein is expressed in the plasma membrane of *Xenopus laevis* oocytes, the Slc10a4 cDNA was extended at the 3′ end by the sequence 5′-gat tac aag gat gac gac gat aag-3′ coding for the FLAG epitope (DYKDDDDK). Sequence insertion was performed by QuikChange site-directed mutagenesis (Stratagene) using the following primers: 5′-cac cca gac ttc cct cga tta caa gga tga cga cga taa gtg atc tag aga ctg aag gag ggt tg-3′ forward and 5′-caa ccc tcc ttc agt ctc tag atc act tat cgt cgt cat cct tgt aat cga ggg aag tct ggg tg-3′ reverse. Sequence verification was carried out by SeqLab Laboratories. For cRNA synthesis, 1 μg of the Slc10a4-FLAG-pBluescript plasmid was linearized with *Xho*I. After phenol/chloroform extraction, DNA was used as a template to generate a 5′-capped cRNA from the T3 promoter.

Immunofluorescence detection of the Slc10a4-FLAG protein in *Xenopus laevis* oocytes

Female *Xenopus laevis* frogs were anesthetized by exposure for 10 min to a 1% solution of 3-aminobenzoic acid ethyl ester (MS-222) (Sigma-Aldrich, Taufkirchen, Germany), and oocytes were prepared as described (Geyer et al., 2004b). After an overnight incubation at 18 °C, defolliculated oocytes were selected and microinjected with 4.6 ng (46 nl) cRNA encoding for the Slc10a4-FLAG protein or with a corresponding 46 nl volume of water. The oocyte medium was changed daily, and intact oocytes were selected for experiments. Three days after cRNA injection, the vitelline membrane was removed, and the oocytes were fixed in a solution of 80% methanol/20% dimethylsulfoxide (v/v). Oocytes were washed in decreasing concentrations of methanol (90%, 70%, 50%, and 30%) in phosphate-buffered saline (PBS; containing 137 mM NaCl, 2.7 mM KCl, 1.5 mM KH_2PO_4, and 7.3 mM Na_2HPO_4, at pH 7.4). They were then incubated with the mouse anti-FLAG antibody (Sigma-Aldrich) overnight at 4 °C in blocking solution (1% bovine serum albumin (BSA) and 4% goat serum in PBS) at a 1:1000 dilution. Oocytes were washed 11 times with PBS and were incubated with the Alexa-Fluor-488-labeled goat anti-mouse immunoglobulin (IgG) secondary antibody (Molecular Probes, Karlsruhe, Germany) at a 1:500 dilution in blocking solution for 2 h at room temperature. After a second washing (6× with PBS), the oocytes were fixed with 3.7% formaldehyde in PBS and dehydrated with increasing concentrations of ethanol (30%, 50%, 70%, and 100%) in PBS. The oocytes were embedded in Technovit 7100 (Heraeus Kulzer, Wehrheim, Germany), and 5 μm sections were cut. Fluorescence imaging of the Slc10a4-FLAG protein was performed with a Leica DM6000B fluorescence microscope (Leica, Bensheim, Germany) at 488 nm excitation wavelength.

Immunofluorescence detection of the HA-Slc10a4-FLAG protein in HEK293 cells

The Slc10a4-FLAG and Slc10a4 cDNA sequences were excised from the pBluescript plasmid and subcloned into the mammalian expression vector pcDNA5 (Invitrogen, Karlsruhe, Germany)

downstream of the cytomegalovirus (CMV) promoter for expression in human embryonic kidney 293 cells (HEK293). Using the same method as described above for FLAG-tag insertion, the HA epitope (YPYDVPDYA) was inserted between amino acid residues 57 and 58 of the Slc10a4-FLAG protein. This construct is further referred to as HA-Slc10a4-FLAG. The following oligonucleotide sense and antisense primers were used for site-directed mutagenesis: 5′-ctc cga gca tcg gct tct acc cct acg acg tcc ccg act acg cca gtc ccg act tga ccc cg-3′ and 5′-cgg ggt caa gtc ggg act ggc gta gtc ggg gac gtc gta ggg gta gaa gcc gat gct cgg ag-3′, respectively. Correct constructs were selected after DNA sequencing. HEK293 cells were seeded in 24-well plates at a density of 2.5×10^5 cells per well on poly-D-lysine-coated glass coverslips and grown to 80% confluency in antibiotic-free D-MEM/F12 medium (Gibco, Karlsruhe, Germany) supplemented with 10% fetal calf serum (Sigma-Aldrich) and 4 mM L-glutamine. Cells were transfected with 1 μg of HA-Slc10a4-FLAG vector DNA by lipofectamine 2000 reagent, according to the manufacturer's instructions (Invitrogen). The parental pcDNA5 vector lacking any insert was used as the control. After 6 h, the medium was changed to standard medium (D-MEM/F12 supplemented with 10% fetal calf serum, 4 mM L-glutamine, 100 U/ml penicillin, and 100 μg/ml streptomycin). One day after transfection, the cells were washed with PBS, fixed with 2% paraformaldehyde in PBS for 15 min at 4 °C, again washed with PBS, and incubated with 20 mM glycine in PBS for 5 min. Subsequently, a part of the transfected HEK293 cells was permeabilized for 5 min in PBT buffer (0.2% Triton X-100 and 20 mM glycine in PBS) and nonspecific binding sites were blocked with 1% BSA (Roche) plus 4% goat serum (Dako, Glostrup, Denmark) in PBS for 30 min at room temperature. Non-permeabilized cells were not treated with PBT. Then, cells were incubated with the primary antibodies, rabbit anti-FLAG (1:40,000 dilution; Sigma-Aldrich), and mouse anti-HA (1:200 dilution, Roche) in blocking solution overnight at 4 °C. The next day, the cells were washed three times with PBS and incubated with the fluorophor-labeled secondary antibodies: goat Cy3-conjugated anti-rabbit IgG (1:800 dilution, Jackson ImmunoResearch, Cambridgeshire, UK) and goat Alexa-Fluor-488-conjugated anti-mouse IgG (1:200 dilution, Molecular Probes) in blocking solution for 60 min at room temperature. After a final washing step with PBS, the cells were covered with a DAPI/methanol solution containing 1 μg/ml DAPI (Roche) and incubated for 5 min at room temperature. The cells were rinsed with methanol, air dried, and mounted onto slides with Mowiol mounting medium (Calbiochem, Darmstadt, Germany). Immunofluorescence was viewed on a Leica DM6000B fluorescence microscope, and cell images were analyzed with the Leica FW4000 Fluorescence Workstation software (Leica).

Cloning of rat CHT1 and human NTCP for transport measurements

Rat CHT1 and human NTCP cDNAs were cloned for comparative analysis. Briefly, the full open reading frames of CHT1 and NTCP were amplified by RT-PCR from 1 μg rat brain and 1 μg human liver RNA, respectively (Clontech). The following gene-specific primers were used: 5′-tgt gga agg atc ttc acg gta c-3′ forward and 5′-atg ggg tca ttg taa gtt atc ttc-3′ reverse for CHT1, and 5′-gcg gta ccg gat gga ggc cca caa c-3′ forward and 5′-tct ctc gag cta ggc tgt gca ag-3′ reverse for NTCP. PCR amplification was performed using the Expand High Fidelity PCR system (Roche) according to the following thermocycling conditions: one cycle of 94 °C×2 min; 10 cycles of 94 °C×15 s, 65 °C×15 s minus 0.5 °C each cycle, and 72 °C×1 min; 30 cycles of 94 °C×15 s, 60 °C×15 s, and 72 °C×1 min; and a final extension of 72 °C×10 min. The PCR products of the expected size were gel purified and cloned into the pcDNA5 vector downstream of the CMV promoter. Sequence verifications were carried out according to GenBank accession numbers NM_053521 (rat CHT1) and NM_003049 (human NTCP).

Transport studies in transfected HEK293 cells

Transient transfection of HEK293 cells with the Slc10a4-pcDNA5, NTCP-pcDNA5, and CHT1-pcDNA5 constructs was performed as described above. Before starting the transport experiments, transfected cells were washed three times with PBS and preincubated with transport buffer (142.9 mM NaCl, 4.7 mM KCl, 1.2 mM $MgSO_4$, 1.2 mM KH_2PO_4, 1.8 mM $CaCl_2$, and 20 mM Hepes, pH 7.4). Uptake experiments were initiated by replacing the preincubation buffer with 300 μl transport buffer containing the radiolabeled test compound and were performed at 37 °C. For inhibition studies, cells were preincubated with transport buffer containing 1 μM hemicholinium-3 as inhibitor for 10 min and then hemicholinium-3 was maintained during the transport experiment at equal concentration. Uptake studies were terminated by removing the transport buffer and washing five times with ice-cold PBS. Cell monolayers were lysed in 1 N NaOH with 0.1% SDS, and the cell-associated radioactivity was determined in a Wallac 1409 liquid scintillation counter (PerkinElmer). The protein content was determined according to Lowry et al. (1951) using aliquots of the lysed cells with BSA as the standard.

Slc10a4 antibody preparation

The polyclonal rabbit anti-Slc10a4 antiserum used in this study was raised against amino acid residues 422–437 of the deduced Slc10a4 protein sequence (VGTDDLVLMETTQTSL, GenBank accession number AAV80706). The synthetic peptide was coupled via the carboxy-terminal glutamic acid residue to keyhole limpet hemocyanin and used to immunize two rabbits (Eurogentec, Seraing, Belgium). Antigenicity of the rabbit serum was confirmed by ELISA analysis using the synthetic peptide as antigen and the polyclonal antiserum was affinity-purified (Eurogentec).

Western blot analysis

HEK293 cells were grown in six-well plates to 80% confluency and transiently transfected with 4 μg of the Slc10a4-FLAG-pcDNA5 construct or pcDNA5 empty vector as described above. After 24 h, the cells were washed with PBS, lysed in ice-cold RIPA buffer containing 150 mM NaCl, 50 mM Tris–HCl (pH 8.0), 1% Nonidet P-40, 0.5% (w/v) sodium deoxycholic acid, 0.1% (w/v) SDS, and protease inhibitor cocktail (Sigma-Aldrich), and cell lysates were cleared by centrifugation. In a second approach, the Slc10a4-FLAG-transfected HEK293 cells were processed with the Proteo-Extract Native Membrane Protein Extraction Kit (Calbiochem), following the manufacturer's standard protocol. The protein content of both preparations was determined using the BCA Protein Assay Kit (Novagen, Darmstadt, Germany). Samples of 20 μg protein were mixed with Laemmli sample buffer (Sigma-Aldrich), separated on 12% SDS polyacrylamide gel and transferred to Hybond-ECL nitrocellulose membrane (Amersham Biosciences, Freiburg, Germany). Additionally, the ReadyBlot Adult Rat Brain Protein Explorer prefabricated blot (Alpha Diagnostics, San Antonio, TX, USA) was used for Slc10a4 expression analysis in different regions of the rat CNS. All blotted membranes were blocked with blocking solution containing 5% (w/v) ECL-blocking agent (Amersham Biosciences) in TBS-T (137 mM NaCl, 10 mM Tris–HCl, pH 8.0, 0.05% Tween-20). The membranes were then incubated overnight at 4 °C with the mouse anti-FLAG antibody (1:10,000 dilution; Sigma-Aldrich), rabbit anti-Slc10a4 antiserum (1:10,000 dilution), or rabbit anti-actin antiserum (1:500 dilution; Sigma-Aldrich). After washing, the membranes were probed with the appropriate horseradish-peroxidase-labeled secondary antibodies for 60 min at room temperature. Signals were developed using the ECL detection kit and visualized by exposure to Hyperfilm ECL (Amersham Biosciences). The specificity of the affinity-purified anti-Slc10a4 antiserum was verified by preincubation with a 100-fold molar excess of the $Slc10a4_{422-437}$ synthetic peptide,

diluted in TBS-T for 60 min at 4 °C. For reprobing of the Western blotting membranes, the antibodies were removed from the membranes by incubation with stripping buffer containing 2% SDS, 62.5 mM Tris–HCl (pH 6.7), and 100 mM β-mercaptoethanol for 60 min at 50 °C.

Radioimmunoprecipitation

HEK293 cells were seeded in six-well plates at a density of 1.25×10^6 cells/well in antibiotic-free D-MEM medium supplemented with 10% fetal calf serum and 4 mM L-glutamine. The cells were grown to 80% confluency and were transiently transfected with 4 μg of the Slc10a4-FLAG-pcDNA5 construct or the pcDNA5 vector alone per well with Roti-Fect transfection reagent (Roth, Karlsruhe, Germany) according to the manufacturer's instructions. After 16 h, the cells were washed twice with PBS and then starved in methionine-free and cysteine-free D-MEM medium (Sigma-Aldrich) for 1 h. Subsequently, the starving medium was changed, 70 μCi of Pro-mix L-[^{35}S] *in vitro* cell labeling mix (GE Healthcare, Freiburg, Germany) was added per well, and protein labeling occurred during incubation for an additional 3 h at 37 °C, 5% CO_2, and 95% humidity. The cells were washed twice with ice-cold PBS, and the cells of each well were lysed in 500 μl ice-cold RIPA buffer containing protease inhibitor cocktail (Sigma-Aldrich) for 5 min under shaking. Cell lysates were transferred to a microcentrifuge tube and incubated for an additional 30 min under rotation at 4 °C. The samples were centrifuged for 15 min at 4 °C and the supernatant was transferred to a fresh tube. One microliter of the monoclonal mouse anti-FLAG antibody (4 mg protein/ml) or 1 μl of the Slc10a4 antiserum was added per 500 μl lysate and incubated for 1 h under rotation at 4 °C. Afterward, 100 μl of protein A-Sepharose CL-4B (GE Healthcare, 25% suspension in RIPA buffer) was added per 500 μl sample and incubated under rotation at 4 °C. After 1 h, the sepharose beads were precipitated by centrifugation and washed three times with ice-cold RIPA buffer. To elute the precipitated proteins, the sepharose beads were heated in Laemmli-buffer at 65 °C for 10 min, and the samples were separated by 12% SDS-PAGE. The gel was fixed in 30% methanol/10% acetic acid (v/v) for 30 min and soaked in Amersham Amplify (GE Healthcare). The dried gel was exposed to Hyperfilm MP (GE Healthcare) at −80 °C.

Immunohistochemical detection of Slc10a4 expression in the rat CNS

For Slc10a4 immunohistochemistry, male Wistar rats were deeply anesthetized by an i.p. injection of 180 mg/kg sodium-pentobarbital (Nacoren; Merial, Hallbergmoos, Germany). The animals were then perfused transcardially with 500 ml of 0.9% NaCl at a pressure of 120 mm Hg (Transcard-pump; Max-Planck Institute, Bad Nauheim, Germany), followed by 200–300 ml of 4% paraformaldehyde in 0.1 M Sørensen phosphate buffer (PB), pH 7.4, at 4 °C. The brain and spinal cord were quickly dissected and postfixed in the same fixative at 4 °C for 2 h, cryoprotected overnight with 20% sucrose solution and frozen in powdered dry ice. In order to locate Slc10a4 expression throughout the CNS in a first experimental approach, serial coronal sections (40 μm) were obtained on a freezing microtome (model 1205; Jung, Heidelberg, Germany). The "free-floating" sections were washed in PB (30 min) and preincubated with PB containing 10% normal horse serum (PAA Laboratories, Linz, Austria) and 0.3% Triton X-100, for 60 min at room temperature. Tissue sections were subsequently incubated for 48 h at 4 °C with the rabbit anti-Slc10a4 antiserum (1:1000 dilution in 2% normal horse serum and 0.1% Triton-X 100 in PB=immunobuffer), rinsed three times (5 min each) with PB, and then transferred to immunobuffer containing biotinylated goat anti-rabbit IgG antiserum at 1:200 dilution (Chemicon, Hampshire, UK) for 60 min at room temperature. Finally, the sections were incubated for 60 min with the avidin/biotin/horseradish peroxidase complex (Vectastain Elite ABC Kit, Linaris Biologische Produkte, Wertheim, Germany), which was visualized by diaminobenzidine hydrochloride (0.5 mg/ml) reaction (Sigma-Aldrich) in the presence of 0.01% hydrogen peroxide. Some sections were counterstained with Cresyl Violet, and coverslips were applied with Entellan (Merck, Darmstadt, Germany) for light microscopic analysis (BX50, Olympus Optical, Hamburg, Germany). To verify specificity of the Slc10a4 antiserum, control experiments were performed with preabsorption of the antiserum with 100-fold molar excess of the synthetic $Slc10a4_{422-437}$ antigen (30 min) prior to the immunohistochemical protocol.

Co-localization studies with ChAT, VAChT, and CHT1

Double immunofluorescence experiments were performed to elucidate the putative co-localization of Slc10a4 with established cholinergic marker proteins (ChAT, VAChT, and CHT1). Serial coronal tissue sections (16 μm) of the whole brain and the spinal cord as well as sections of the intestine (proximal duodenum, terminal ileum, and distal colon) were obtained with a cryostat (model HM-500-O, Microm, Walldorf, Germany) at −20 °C and mounted on poly-L-lysine coated slides. The preincubation was carried out as described above, and the slide-attached tissue sections were uniformly overlaid with immunobuffer containing the rabbit anti-Slc10a4 antiserum (dilution 1:1000) in combination with either goat anti-VAChT antiserum (1:1000 dilution; Chemicon), mouse anti-CHT1 antibody (1:500 dilution; Chemicon), or mouse anti-ChAT antibody (1:250 dilution; Chemicon) in a humidified chamber at 4 °C for 48 h. The slides were rinsed in PB (3×5 min) and incubated for 2 h at room temperature with the secondary antibodies, Cy3-conjugated donkey anti-rabbit IgG (1:800 dilution; Dianova, Hamburg, Germany) and either Alexa-Fluor-488-conjugated donkey anti-goat IgG (1:500 dilution; Sigma-Aldrich) or Alexa-Fluor-488-conjugated goat anti-mouse IgG (1:500 dilution; Sigma-Aldrich). After washing steps with PB, the tissues were coverslipped with Citifluor. The primary anti-Slc10a4 antiserum employed was tested for specificity by preincubation with the Slc10a4 antigen (see above). Omission of the antigen-specific primary antisera was used as a further immunohistochemical control experiment for each antiserum/antibody. Tissue sections were analyzed with an Olympus BX50 microscope equipped with appropriate filter sets, a spot-insight B/W digital camera (Visitron Systems; Puchheim, Germany), and the image editing software MetaMorph 5.05 (Universal Imaging Corporation, West Chester, PA, USA).

Sequence analysis

Membrane topology and putative membrane-spanning domains were calculated by the following programs: HMMTOP, TMpred, TMHMM, MEMSAT, PRED-TMR2, and TMAP. The NetNGlyc 1.0 program was used to predict N-linked sites and NetPhos 2.0 was used to predict potential phosphorylation sites in the Slc10a4 protein.

Statistical analysis

Statistical significance for uptake measurements with radiolabeled substrates was calculated by one-way analysis of variance (ANOVA) followed by post hoc testing (Dunnett).

RESULTS

Cloning of rat Slc10a4

In 2004, a cDNA sequence (GenBank accession number XM_579196) was predicted by automated computational analysis from the rat genome that showed sequence identity of about 30% to the bile acid carriers Ntcp and Asbt as

well as about 82% sequence identity to a human cDNA clone that was unassigned at that time (GenBank accession number BC012048), but that was later annotated as SLC10A4. Using an RT-PCR based approach for cloning, a 1314-bp transcript was obtained from the rat adrenal gland. This sequence was deposited into the GenBank database with accession number AY825923 (release date December 6th, 2004). The cloned transcript codes for a 437 amino acid protein with a calculated molecular mass of 46.6 kDa; it is referred to as rat Slc10a4 protein. This protein shows 85% sequence identity to the human SLC10A4 protein (GenBank accession number NP_689892) (Fig. 1) and 95% sequence identity to the mouse Slc10a4 protein (GenBank accession number NP_775579). Amino acid sequence alignment revealed highly conserved domains with the other rat Slc10 carrier proteins Ntcp, Asbt, and Soat. However, the highly conserved "ALGMMPL" signature motif of all NTCP/Ntcp, ASBT/Asbt, and SOAT/Soat proteins (Geyer et al., 2006) was not present in the rat Slc10a4 and human SLC10A4 protein sequences. Furthermore, the length of the N-terminal domain of the SLC10A4/Slc10a4 proteins clearly exceeded those of Ntcp, Asbt, and Soat by ~60 amino acids (Fig. 1). According to the prediction from bioinformatic programs outlined in the Experimental Procedures section, several potential outer facing N-glycosylation sites (residues Asn^{6}, Asn^{20}, Asn^{26}, Asn^{181}, and Asn^{195}) and potential inner facing phosphorylation sites (Ser^{405}, Thr^{417}, and Y^{419}) occur in the rat Slc10a4 protein. All of these N-glycosylation and phosphorylation sites are conserved among the rat Slc10a4 and the human SLC10A4 proteins.

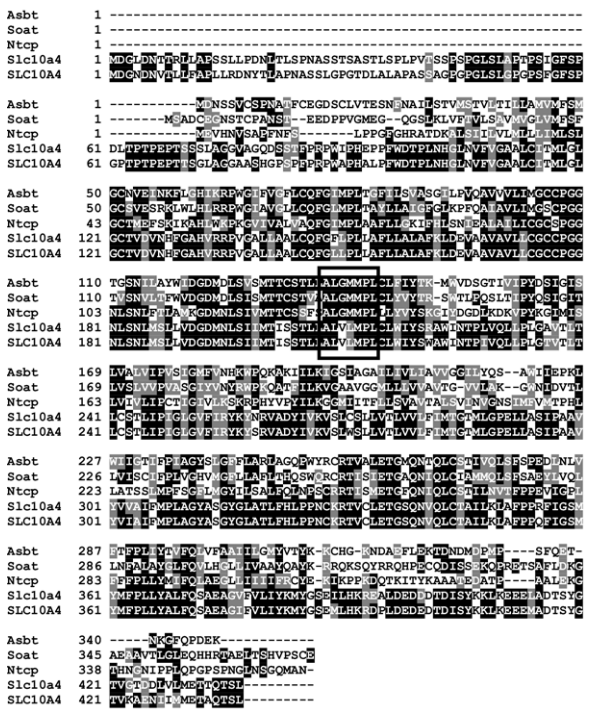

Fig. 1. Amino acid sequence alignment of the rat Slc10 carrier proteins Asbt (Slc10a2), Soat (Slc10a6), Ntcp (Slc10a1), and Slc10a4, as well as human SLC10A4. The alignment was conducted using the *ClustalW* algorithm and was visualized by BOXSHADE 3.21. The amino acid sequence identities are displayed with black shading; amino acid similarities are highlighted in gray. Gaps (−) are introduced to optimize alignment. The signature motif of all NTCP/Ntcp, ASBT/Asbt, and SOAT/Soat proteins is highlighted.

Expression analysis of SLC10A4/Slc10a4 mRNAs in human, rat, and mouse tissues

Expression analysis of human SLC10A4 mRNA and of rat and mouse Slc10a4 mRNAs was performed with quantitative real-time PCR. For the rat, Slc10a4 expression was highest in the brain and was moderate in the adrenal gland, from which Slc10a4 was originally cloned. In contrast, very low Slc10a4 mRNA expression levels were detected in heart, kidney, spleen, testis, lung, skeletal muscle, pancreas, stomach, small intestine, and colon (Fig. 2A). Mouse Slc10a4 mRNA expression was also highest in the brain and significantly above background levels in the eye, prostate, and whole embryo tissue preparations (Fig. 2B). With regard to human tissues, SLC10A4 mRNA was highly expressed in brain and small intestine, and moderately expressed in colon, heart, prostate, and testis. Very low levels of human SLC10A4 mRNA were detected in kidney, liver, ovary, placenta, spleen, and thymus (Fig. 2C).

Transport studies and membrane expression of the rat Slc10a4 protein

Because of the close phylogenetic relationship between Slc10a4 and the liver bile acid carrier Ntcp, transport experiments were performed in Slc10a4 transfected HEK293 cells using the radiolabeled Ntcp substrates, taurocholate and estrone-3-sulfate. The neurosteroids DHEAS and pregnenolone sulfate (PREGS) were also included in the transport measurements. In all transport experiments, we used the human NTCP carrier as the positive control. In contrast to human NTCP, no specific Slc10a4-mediated transport activity was observed for these compounds (Table 1). Identical results were obtained in NTCP-expressing and Slc10a4-expressing *Xenopus laevis* oocytes (data not shown). A FLAG-tagged Slc10a4 protein was generated and expressed in *Xenopus laevis* oocytes, in order to exclude the possibility that the absence of Slc10a4-specific transport activity might have been due to a defect in its functional expression at the plasma membrane. Membrane localization of the fusion protein was analyzed with a FLAG-specific monoclonal antibody by immunofluorescence microscopy and revealed that Slc10a4 expression in the oocytes was clearly directed to the plasma membrane (Fig. 3A). Membrane topology of the Slc10a4 protein was analyzed by six different topology prediction programs. Controversial protein structures with either seven or eight transmembrane domains (TMDs) were obtained. The TMpred and MEMSAT programs placed the N-terminus and C-terminus at the extracellular compartment and predicted eight TMDs; the HMMTOP and TMHMM programs also predicted eight TMDs but with an intracellular localization of both terminals. In contrast, PRED-TMR2 and TMAP predicted seven TMDs with an extracellular localization of the N-terminus and an intracellular C-terminus (Fig. 3B). In

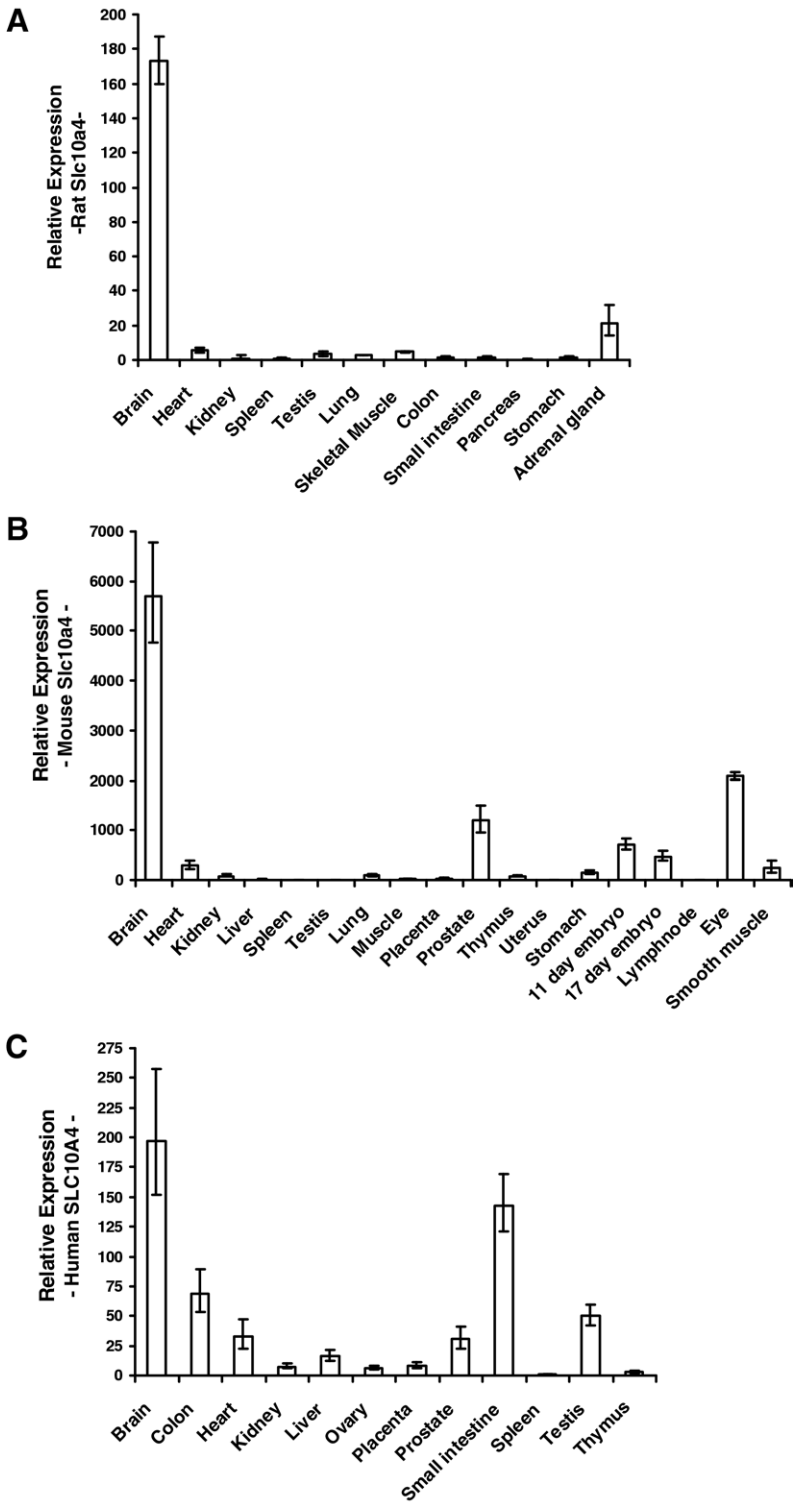

Fig. 2. Expression patterns of rat and mouse Slc10a4 mRNAs (A+B) and human SLC10A4 mRNA (C) analyzed by real-time quantitative PCR. Relative expression was calculated by $2^{-\Delta\Delta CT}$ transformation and represents x-fold higher SLC10A4/Slc10a4 expression in the respective tissue as compared with the organ of lowest expression among each panel. Data represent means±S.D. of quadruplicate measurements.

order to experimentally clarify the membrane topology of Slc10a4, a second Slc10a4-tagged protein, HA-Slc10a4-FLAG, was generated containing the hemagglutinin (HA) motif at its N-terminal end in addition to the C-terminal FLAG-motif. This fusion protein was expressed in HEK293 cells, and the accessibility of the HA-directed and FLAG-

Table 1. Transport studies with rat Slc10a4 and human NTCP in HEK293 cells

Test compound	NTCP		Slc10a4	
	Uptake (pmol/mg protein/10 min)	Ratio	Uptake (pmol/mg protein/10 min)	Ratio
Taurocholate [1 μM]	239.61±26.47	40.3*	7.03±0.68	1.2
Estrone-3-sulfate [1 μM]	47.95±6.61	6.1*	9.60±2.72	1.2
DHEAS [1 μM]	62.63±13.93	4.5*	21.15±3.24	1.5
PREGS [1 μM]	663.78±81.49	2.9*	216.51±18.6	1.0

HEK293 cells were seeded in 24-well plates and transfected with the Slc10a4-pcDNA5 and NTCP-pcDNA5 constructs. HEK293 cells transfected with the empty pcDNA5 vector were used as the control. Cells were incubated with the indicated radiolabeled compound for 10 min and cell-associated radioactivity was measured and calculated as the ratio value when compared to transport under control conditions. The values represent means±S.D. of triplicate determinations of representative experiments.

* $P<0.01$, significantly higher uptake into NTCP-pcDNA5 transfected HEK293 cells compared with empty pcDNA5 vector-transfected HEK293 cells.

directed antibodies to their respective epitopes was analyzed by immunofluorescence under membrane permeabilizing and non-permeabilizing conditions. While the antibodies reached both epitopes in the permeabilized cells, the HA epitope but not the FLAG epitope was detectable under non-permeabilizing conditions (Fig. 3C). This data strongly support a 7-TMD model for the rat Slc10a4 protein with a N_{exo}/C_{cyt} *trans*-orientation of the N- and C-terminal domains. Closer analysis of this immunofluorescence data showed that although Slc10a4 was detected at the plasma membrane of HEK293 cells, it was also detectable in intracellular compartments of yet unknown origin (Fig. 3C).

Antibody preparation and Western blot analysis

In order to analyze macroscopic brain-region specific localization and microscopic cellular localization of Slc10a4 expression in the rat CNS, immunohistochemistry was performed with a polyclonal rabbit antiserum directed against the C-terminal epitope VGTDDLVLMETTQTSL (amino acid residues 422–437) of the rat Slc10a4 protein. The specificity of this antiserum was verified by Western blot analysis of Slc10a4-FLAG transfected HEK293 cells. A specific band of ~48 kDa was detected in cell lysates of the Slc10a4-FLAG transfected cells, but not in the mock-transfected cells, when employing the anti-Slc10a4 antiserum and the anti-FLAG antibody (Fig. 4A, upper panel). This band fits the predicted molecular weight of Slc10a4 of 46.6 kDa plus the molecular weight of the FLAG epitope of 1 kDa. In cells transfected with the untagged Slc10a4 protein, a smaller band of ~47 kDa was found, that appeared only after incubation with the Slc10a4 antiserum but not with the anti-FLAG antibody. When the transfected cells were processed with the ProteoExtract Native Membrane Protein Extraction method, the Slc10a4 protein was enriched in the membrane protein fraction, but was not detectable in the soluble protein fraction. In order to reveal epitope specificity, preabsorption of the Slc10a4 antiserum and the anti-FLAG antibody with a 100-fold molar excess of the synthetic $Slc10a4_{422-437}$ immunizing peptide was performed. This preincubation substantially suppressed immunostaining with the Slc10a4 antiserum but did not affect immunostaining with the anti-FLAG antibody (Fig. 4A, lower panel). In a second approach, the Slc10a4-FLAG protein was separated by radioimmunoprecipitation with the anti-Slc10a4 antiserum and the anti-FLAG antibody, and in both cases revealed a single band at ~48 kDa that was not present in the mock-transfected control cells (Fig. 4B).

The Slc10a4 antiserum was also used for Western blot analysis of various regions of the rat CNS (Fig. 4C). Analogous to the Slc10a4 transfected HEK293 cells, a specific band was detected at ~47 kDa that most likely represents the native form of the protein. Additionally, a second band was present at ~73 kDa in almost all brain regions that was completely abolished by preincubation of the Slc10a4 antiserum with the synthetic $Slc10a4_{422-437}$ immunizing peptide (Fig. 4C, lower panel). Among the brain regions investigated, the caudate putamen exhibited the highest levels of immunoreactivity; whereas, only a faint band was detectable in the cerebellum. The frontal cortex, posterior cortex, hippocampus, olfactory bulb, thalamus, mesencephalon, entorhinal cortex, pons, medulla oblongata, and spinal cord showed intermediate levels of Slc10a4 immunoreactivity.

Immunohistochemical analysis of Slc10a4 expression in the rat CNS

Using 40 μm floating sections of the rat brain and spinal cord, substantial Slc10a4-like immunoreactivity was detectable in all areas commonly described as cholinergic regions. There we found Slc10a4-immunopositive perikarya and dendrites, as well as fibers, varicosities, and synaptic puncta. The results of these localization studies are summarized in Table 2. Labeling for Slc10a4 was visualized along nerve fibers in the cerebral cortex, notably in the cingulate, prelimbic, infralimbic, and dorsal peduncular cortex. A high density of Slc10a4-immunopositive perikarya and puncta was identified in the islands of Calleja, the nucleus of the horizontal limb of the diagonal band of Broca (Fig. 5A), the olfactory tubercle (Fig. 5B), and the accumbens nucleus (Fig. 5C). The caudate putamen exhibited strong puncta-directed immunoreactivity; whereas, Slc10a4-like staining of cell bodies was scarce in this area (Fig. 5D). Only a few Slc10a4 positive perikarya were detectable in the basal nucleus of Meynert; whereas, the amygdala was densely innervated by Slc10a4-positive fibers, particularly the basolateral amygdaloid nucleus (Fig. 5E). In the hippocampus, the field CA3 presented a higher density of

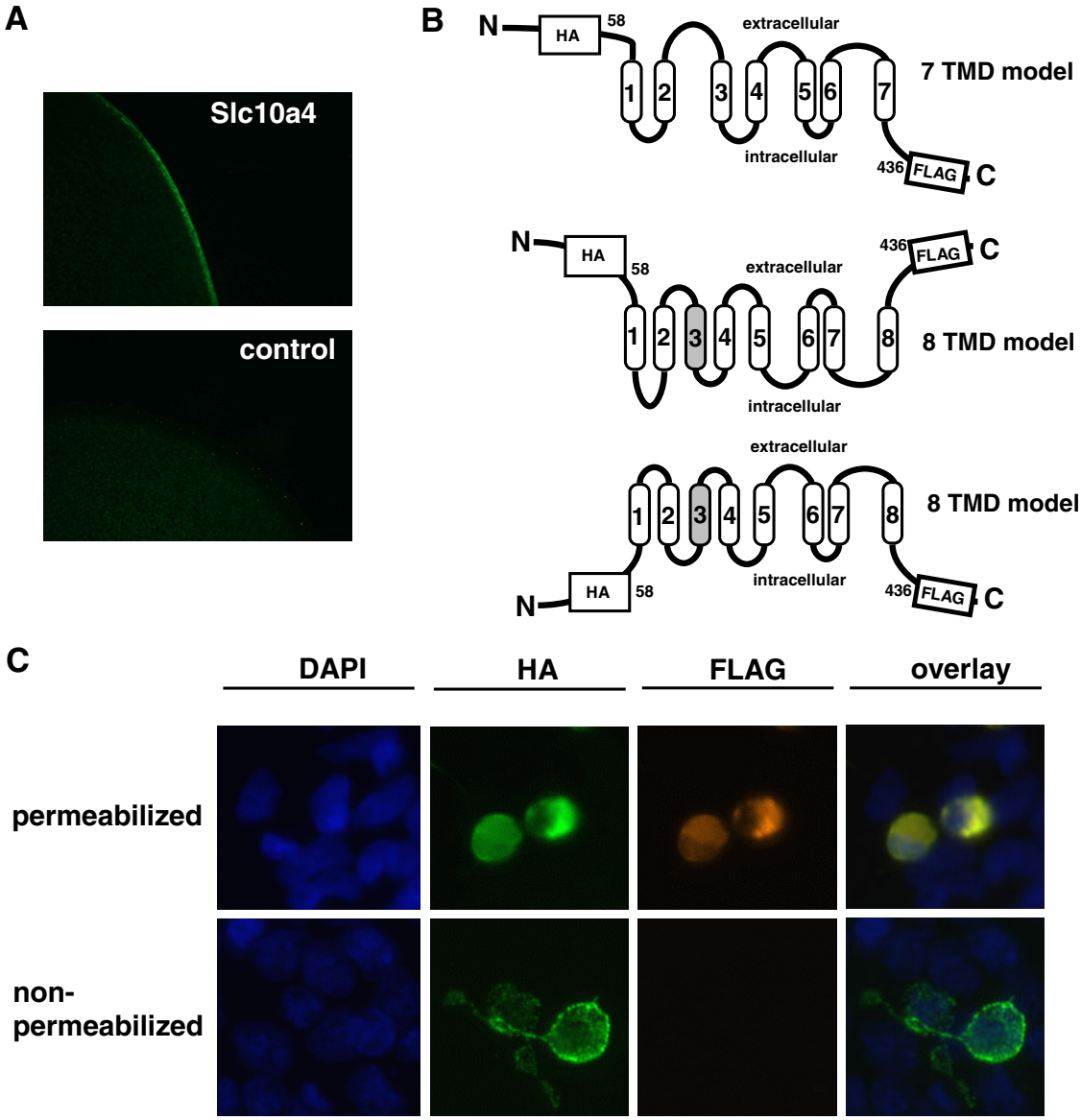

Fig. 3. Membrane expression and topology of the rat Slc10a4 protein. (A) Detection of the Slc10a4-FLAG fusion protein in the plasma membrane of *Xenopus laevis* oocytes. Oocytes were injected with 4.6 ng (in 46 nl) of Slc10a4-FLAG-cRNA or 46 nl water (control). After 3 days in culture oocytes were fixed and processed for immunofluorescence microscopy. (B) Proposed membrane topologies of the rat Slc10a4 protein, based on the analysis of six different topology prediction programs for eukaryotic proteins (see text for further explanations). Cylinders indicate predicted TMDs, and loops are depicted as lines. Strategically inserted FLAG and HA epitopes are illustrated as boxes. Amino acid positions immediately preceding these tags are indicated. Experimental data clearly support the 7-TMD model for the rat Slc10a4 protein. (C) Detection of the HA-Slc10a4-FLAG double-tagged protein by immunofluorescence microscopy. HEK293 cells were transfected with the HA-Slc10a4-FLAG construct and were analyzed under permeabilized and non-permeabilized conditions. Expression of the tagged proteins was detected by fluorescence labeling using a mouse anti-HA monoclonal primary antibody followed by Alexa-Fluor-488-conjugated anti-mouse IgG secondary antibody (green fluorescence) and rabbit anti-FLAG polyclonal primary antiserum followed by Cy3-conjugated anti-rabbit secondary antibody (orange fluorescence). Nuclei were stained with DAPI.

Slc10a4-positive puncta than CA1. A similar staining pattern of Slc10a4 was found in the granular layer of the dentate gyrus. Slc10a4-positive fibers and nerve terminals were also widespread in the thalamus and epithalamus, especially in the reticular thalamic nucleus and medial habenular nucleus. In the latter region, we also found somesmall Slc10a4-immunoreactive cell bodies. Additionally, immunoreactive puncta and perikarya were visualized in many regions of the mesencephalon, such as the laterodorsal tegmental nucleus, pedunculopontine tegmental nucleus, periaqueductal gray, oculomotor nucleus, interpeduncular nucleus, ventral tegmental area, and substantia nigra (SN) (the latter region is shown in Fig. 5F). Positive immunoreactive cell bodies and puncta were also detected in the rhombencephalon, especially in the motor trigeminal nucleus, the facial nucleus (Fig. 5G), the dorsal motor nucleus of vagus (Fig. 5H), the hypoglossal nucleus (Fig. 5I), and the ambiguus nucleus (Fig. 5J). In these

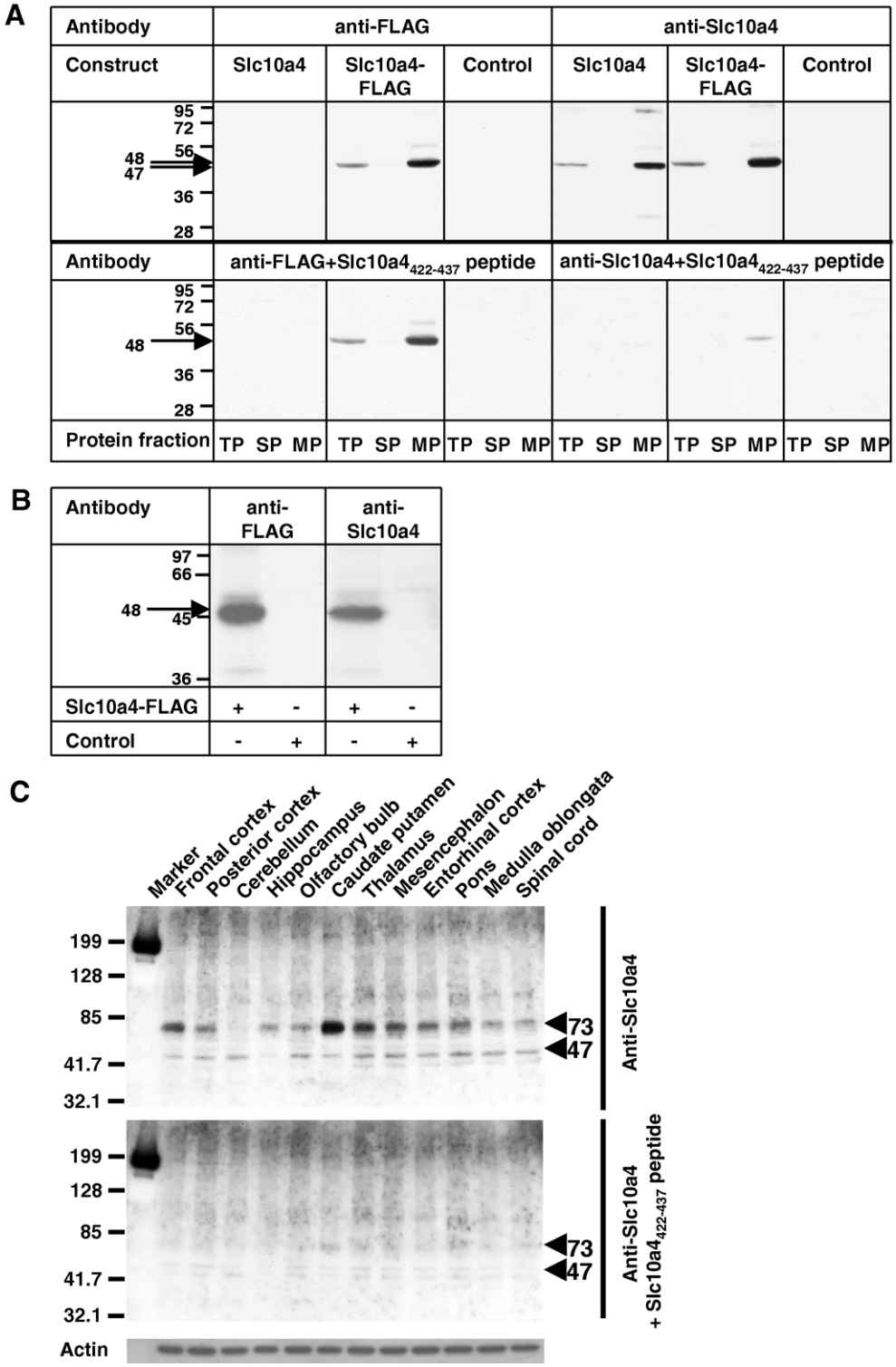

Fig. 4. Western blot analysis (A) and radioimmunoprecipitation (B) of cell lysates of Slc10a4-FLAG and Slc10a4 transfected HEK293 cells, and (C) Western blot analysis of different regions of the rat CNS. (A, B) HEK293 cells were transiently transfected with the Slc10a4-FLAG-pcDNA5 and Slc10a4-pcDNA5 constructs or empty pcDNA5 vector (control). (A) Proteins from total cell lysates (TP), soluble protein fractions (SP), and membrane protein fractions (MP) were prepared from these cells and separated on 12% SDS-polyacrylamide gel. Western blotting with the Slc10a4 antiserum and the anti-FLAG antibody revealed a single dominant band at ~48 kDa and ~47 kDa for the FLAG-tagged and the untagged Slc10a4 protein, respectively (A, upper panel). Preincubation of the Slc10a4 antiserum with the $Slc10a4_{422-437}$ immunizing peptide substantially suppressed immunostaining. In contrast, immunostaining with the anti-FLAG antibody was not affected by preincubation with the Slc10a4 antigen (A, lower panel). (B) Radioimmunoprecipitation of the Slc10a4-FLAG protein by employing the Slc10a4 antiserum and the anti-FLAG antibody revealed a single band at ~48 kDa. (C) A pre-manufactured membrane with adsorbed protein extracts of various regions of the rat CNS (Alpha Diagnostics) was probed with the anti-Slc10a4 antiserum and showed bands at ~47 kDa and ~73 kDa (upper panel), which were substantially suppressed after preincubation of the Slc10a4 antiserum with the synthetic $Slc10a4_{422-437}$ peptide (lower panel). Detection of actin was performed for loading control of the pre-fabricated blot.

Table 2. Regional distribution of Slc10a4, VAChT, and CHT1 immunoreactivities in the rat CNS

Brain regions	Immunoreactivities					
	Density of perikarya			Density of puncta/fibers		
	Slc10a4	VAChT	CHT1	Slc10a4	VAChT	CHT1
Cortex						
Cingulate cortex (Cg)	−	−	−	+	+	+
Prelimbic cortex (PrL)	−	−	−	+	+	+
Infralimbic cortex (IL)	−	−	−	+	+	+
Dorsal peduncular cortex (DP)	−	−	−	+	+	+
Olfactory system						
Olfactory bulb (OB)	−	−	−	+	+	++
Olfactory tubercle (Tu)	++	++	++	+++	+++	+++
Septal/basal forebrain						
Islands of Calleja (ICj)	++	++	++	+++	+++	+++
Horizontal limb of the diagonal band (HDB)	+++	+++	+++	++	++	++
Vertical limb of the diagonal band (VDB)	+	+++	+++	+	+++	+++
Medial septal nucleus (MS)	+	+++	+++	+	+	+
Lateral septal nucleus (LS)	−	−	−	+	++	++
Accumbens nucleus (Acb)	++	++	++	++	++	++
Caudate putamen (striatum) (CPu)	+	++	+++	++	+++	+++
Basal nucleus (Meynert) (B)	+	+++	+++	+	+	+
Amygdala						
Lateral amygdaloid nucleus (La)	−	−	−	+	+	+
Basolateral amygdaloid nucleus (BL)	−	−	−	+++	++	++
Hippocampus						
Fimbria of the hippocampus (fi)	−	−	−	++	++	++
Septofimbrial nucleus (Sfi)	−	−	−	++	++	++
Field CA1 of the hippocampus (CA1)	−	−	−	+	++	++
Field CA3 of the hippocampus (CA3)	−	−	−	++	+++	++
Granular layer of the dentate gyrus (GrDG)	−	−	−	++	++	++
Thalamus/epithalamus						
Reticular thalamic nucleus (Rt)	−	−	−	+++	++	++
Lateral habenular nucleus (LHb)	−	−	−	+	+	+
Medial habenular nucleus (MHb)	+	+++	++	++	+	+
Anterodorsal thalamic nucleus (AD)	−	−	−	+	+	+
Anteromedial thalamic nucleus (AM)	−	−	−	+	+	+
Anteroventral thalamic nucleus (AV)	−	−	−	+	+++	++
Mediodorsal thalamic nucleus (MD)	−	−	−	+	+	+
Paraventricular thalamic nucleus (PV)	−	−	−	+	+	+
Reuniens thalamic nucleus (Re)	−	−	−	+	+	+
Central medial thalamic nucleus (CM)	−	−	−	+	++	+
Mesencephalon						
Superior colliculus (SC)	−	−	−	++	+	+
Edinger-Westphal nucleus (EW)	−	−	−	+	+	+
Laterodorsal tegmental nucleus (LDTg)	++	+++	+++	+	+	+
Pedunculopontine tegmental nucleus (PPTg)	++	+++	+++	+	+	+
Periaqueductal gray (PAG)	++	−	−	++	+	+
Oculomotor nucleus (3N)	++	+++	+++	++	+	++
Interpeduncular nucleus (IP)	+	−	−	+	+++	+++
Ventral tegmental area (VTA)	+	−	−	+++	+	+
Substantia nigra (SN)	++	−	−	++	−	−
Parabigeminal nucleus (PBG)	++	++	++	−	−	−
Rhombencephalon						
Pontine nuclei (Pn)	−	−	−	+	++	+
Dorsal raphe nucleus (DR)	−	−	−	+	+	+
Ventral tegmental nucleus (VTg)	−	−	−	+	+	+
Raphe pallidus nucleus (RPa)	−	−	−	+	+	+
Spinal trigeminal nucleus (Sp5)	−	−	−	++	++	++
Motor trigeminal nucleus (5N)/peritrigeminal zone (P5)	+++	+++	+++	+++*	+++*	++*
Paratrigeminal nucleus (Pa5)	−	−	−	+	+	+
Vestibular nuclei (Ve)	−	−	−	++	+	+
Facial nucleus (7N)	+++	+++	+++	++*	++*	++*

Table 2. continued

Brain regions	Immunoreactivities					
	Density of perikarya			Density of puncta/fibers		
	Slc10a4	VAChT	CHT1	Slc10a4	VAChT	CHT1
Nucleus of the solitary tract (Sol)	−	−	−	++	+	+
Dorsal motor nucleus of vagus (10N)	++	+++	++	++	−	−
Hypoglossal nucleus (12N)	+++	+++	+++	++*	++*	++*
Ambiguus nucleus (Amb)	+++	+++	+++	+++*	++*	++*
Lateral reticular nucleus (LRt)	−	−	−	+	+	+
Spinal cord						
Cervical and thoracic, layer IX	+++	+++	++	+++*	+++*	++*
Cervical and thoracic, layer III	−	−	−	++	+	+

The densities of Slc10a4, VAChT, and CHT1 immunopositive perikarya or puncta/fibers were rated as follows: "−," absent; "+," low; "++," moderate; "+++," high. In several cranial motor nuclei and the spinal cord, puncta represent synaptic C-boutons as indicated by asterisks (*). Brain regions and structures were attributed and named according to Paxinos and Watson (2004).

regions, neurons were surrounded by Slc10a4-positive puncta, possibly representing synaptic C-boutons. This staining pattern was also found in layer IX of the spinal cord. There, positive staining of fibers was also visualized in layer III of the dorsal horn (Fig. 5K).

Co-localization studies with VAChT, CHT1, and ChAT

Because the immunohistochemically identified Slc10a4 distribution pattern indicated its expression in cholinergic regions, nuclei or even neurons in the rat CNS, co-localization studies were performed for Slc10a4 immunoreactivity and that of three different marker proteins of cholinergic neurons, namely VAChT, CHT1, and ChAT. Significant immunoreactive co-labeling of neuronal perikarya and nerve terminals was found for Slc10a4 and VAChT (Fig. 6A–C) as well as for Slc10a4 and CHT1 (Fig. 6D–F) by fluorescence microscopy in all cholinergic nuclei and their projections, such as the islands of Calleja (Fig. 6A), the accumbens nucleus (Fig. 6B), the olfactory tubercle (Fig. 6D), and the horizontal limb of the diagonal band of Broca (Fig. 6E). Furthermore, clear synaptic co-expression of Slc10a4 and VAChT as well as of Slc10a4 and CHT1 was observed in motor neurons of the ventral horn of the spinal cord (Fig. 6C) and in the motor trigeminal nuclei (Fig. 6F), respectively. Visualization of Slc10a4-immunopositive neurons proved to be scarce, however, throughout the vertical limb of the diagonal band of Broca, the medial septal nucleus, the caudate putamen and the basal nucleus of Meynert, when compared with immunolabeling for CHT1 or VAChT (Table 2). In contrast, nerve fiber systems within the basolateral amygdaloid nucleus and the dorsal motor nucleus of the vagus revealed stronger specific immunoreactivity for Slc10a4 than for VAChT or CHT1 (Table 2). Numerous Slc10a4-immunoreactive cell bodies and puncta were also demonstrated in the ventral tegmental area and the SN, but these were not clearly labeled for the cholinergic marker proteins VAChT and CHT1. Therefore, additional co-labeling experiments were performed for Slc10a4 and the cholinergic marker protein ChAT in order to clarify the origin of Slc10a4 expression in these areas. A significant number of both Slc10a4 and ChAT immunopositive cell bodies at very high degree of co-localization was detected in the ventral tegmental area (Fig. 6G) and detailed analysis revealed an intracellular compartmentalization of both proteins (Fig. 6H). Also within cell bodies of the SN, Slc10a4-immunoreactivity proved to be co-localized with that of ChAT-immunoreactivity (Fig. 6I). Apart from the CNS, immunohistochemical studies were also performed on tissue sections of various intestinal regions, namely the proximal duodenum, terminal ileum, and distal colon. In all sections, Slc10a4-immunoreactivity was detected in neuronal cell bodies and fibers of the myenteric plexus as part of the enteric nervous system, where it was clearly co-localized with VAChT-immunoreactivity (Fig. 7).

Transport studies with [^{3}H]choline chloride

As the proteins most related to Slc10a4 are membrane carriers, we speculated that besides the hemicholinium-3 sensitive choline transporter CHT1, Slc10a4 might also be involved in choline reuptake in the presynaptic membrane of cholinergic synapses. To test this hypothesis, we transiently transfected Slc10a4 and CHT1 into HEK293 cells and performed transport experiments with [^{3}H]choline chloride (1 μM) in the presence and absence of 1 μM hemicholinium-3 as an inhibitor. In contrast to CHT1 though, which showed hemicholinium-3 sensitive choline chloride transport as described (Ribeiro et al., 2003), Slc10a4-specific transport activity for [^{3}H]choline chloride was not detected in these transfected cells (Fig. 8).

DISCUSSION

The Slc10a4 protein characterized in the present study belongs phylogenetically to the SLC10 carrier family of "sodium/bile acid cotransporters" (Hagenbuch and Dawson, 2004; Geyer et al., 2006). The founding members of this family (Ntcp and Asbt) have been known since 1990 to maintain the enterohepatic circulation of bile acids between the liver and the gut (Meier and Stieger, 2002). The novel SLC10 members, SLC10A4 (man) and Slc10a4 (rat and mouse), have their highest mRNA expression levels in the brain, according to quantitative real-time PCR analysis

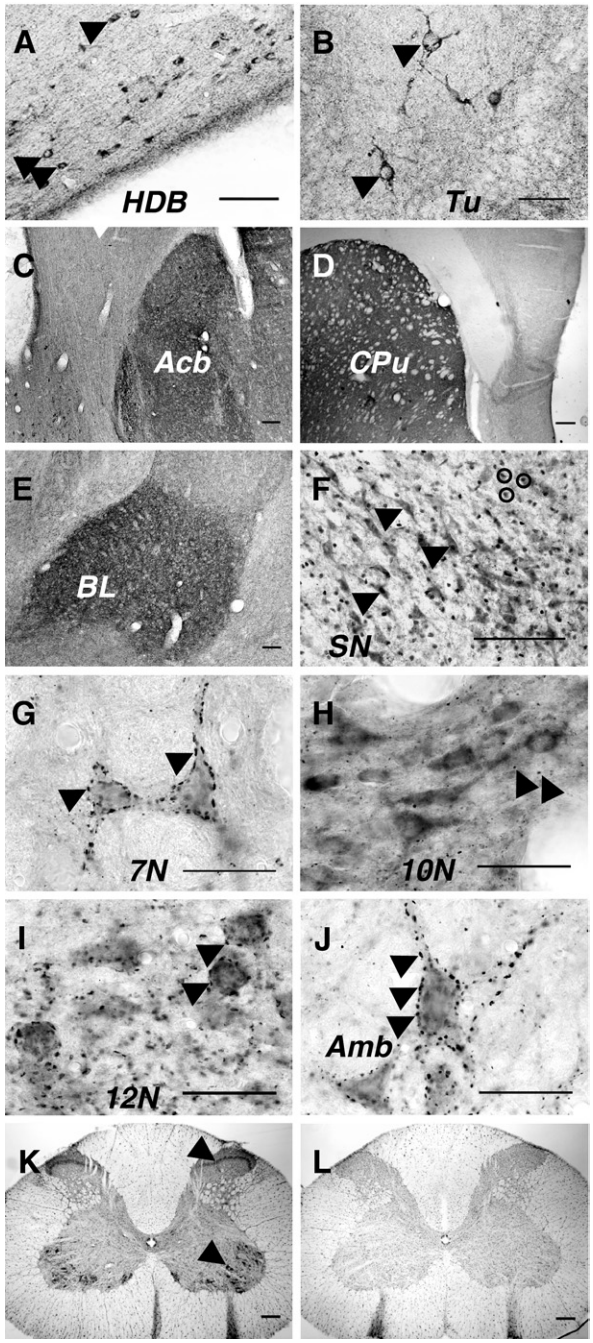

Fig. 5. Light microscopic distribution of Slc10a4-like immunoreactivity in the rat CNS. Coronal sections (40 μm) of the rat CNS were incubated with the Slc10a4-antiserum and processed for indirect immunohistochemical staining according to the DAB technique. Labeled cell bodies (indicated by arrows) and puncta are present in (A) the nucleus of the horizontal limb of the diagonal band of Broca (HDB) and (B) the olfactory tubercle (Tu). In (C) the accumbens nucleus (Acb) and (D) the caudate putamen (CPu), dense immunolabeling for the Slc10a4 protein was seen. (E) Slc10a4-immunoreactive puncta and fibers are stained in the basolateral amygdaloid nucleus (BL). (F) Slc10a4-containing perikarya were found within the SN; neurons are marked by arrows, and nuclei counterstained with Cresyl Violet are indicated by small circles. (G–J) Slc10a4-immunopositive cell bodies and puncta (indicated by arrows) were stained in the medullary motor nuclei such as the facial nucleus (7N), the dorsal motor nucleus of vagus (10N), the hypoglossal nucleus (12N), and the ambiguus nucleus (Amb). (K) In the spinal cord, Slc10a4-containing cell bodies and puncta are present in the ventral horn (layer IX, indicated by arrow), whereas only fibers are visualized in the dorsal horn (layer III, indicated by arrow). (L) A section from the spinal cord was incubated with the Slc10a4 antiserum preabsorbed with the $Slc10a4_{422-437}$ immunizing peptide and showed pronounced reduction in immunoreactivity. Brain regions and structures were attributed and abbreviated according to Paxinos and Watson (2004). Scale bars=100 μm (A, C, E, F); 50 μm (B, G–J); 200 μm (D, K–L).

(Fig. 2). This agrees with several EST sequences (GenBank accession numbers BE260783, BF312464, BI198043) and full insert cDNA sequences (GenBank accession numbers AK126542, BC012048, BC019066) related to the human SLC10A4 transcript that all derived from brain neuroblastoma. High SLC10A4 mRNA levels were detected in the human brain by Northern blot analysis also in a recent study by Splinter and coworkers (2006). Cellular localization of the SLC10A4/Slc10a4 protein in particular for the brain though remained unknown. We therefore attempted to localize for the first time the rat Slc10a4 protein within central nervous structures using a polyclonal rabbit antiserum directed against the C-terminus of the rat Slc10a4 protein. The specificity of this antiserum was verified by Western blot analysis and immunoprecipitation experiments with Slc10a4 transfected HEK293 cells, that revealed a single dominant band at ~48 kDa and ~47 kDa for the Slc10a4-FLAG protein and the untagged Slc10a4 protein, respectively. This band disappeared after preincubation of the Slc10a4 antiserum with the immunizing peptide, thus indicating epitope specificity.

Using this antiserum, Slc10a4 proved to be expressed in all cholinergic cell groups and their projection pathways in the rat brain, commonly identified by ChAT expression (Eckenstein and Thoenen, 1982; Armstrong et al., 1983; Levey et al., 1983a,b) and immunoreactivities for VAChT (Gilmor et al., 1996; Weihe et al., 1996) or CHT1 (Misawa et al., 2001; Ferguson et al., 2003; Kus et al., 2003). Slc10a4-directed immunoreactivity was detected in perikarya and/or nerve terminals at varying degree in all of these cholinergic regions. A detailed overview of all brain regions that show expression of Slc10a4, CHT1, or VAChT is given in Table 2.

Lein and coworkers (2007) just recently published the expression pattern of more than 20,000 genes in the adult mouse brain, including Slc10a4, that were generated by automated high-throughput *in situ* hybridization and are organized in the Allen Brain Atlas (online under www.brain-map.org). Data obtained from this atlas clearly show that the mouse Slc10a4 gene is highly transcribed in cholinergic regions such as the caudate-putamen, olfactory tubercle, diagonal band of Broca, laterodorsal tegmental nucleus, pedunculopontine tegmental nucleus, and cranial nerve nuclei. Additionally, the atlas shows strong hybridization signals in the SN and ventral tegmental area. This pattern fully matches the immunohistochemical localization data of the rat Slc10a4 protein provided in the present study, thereby strongly supporting the specificity of the Slc10a4 antiserum used.

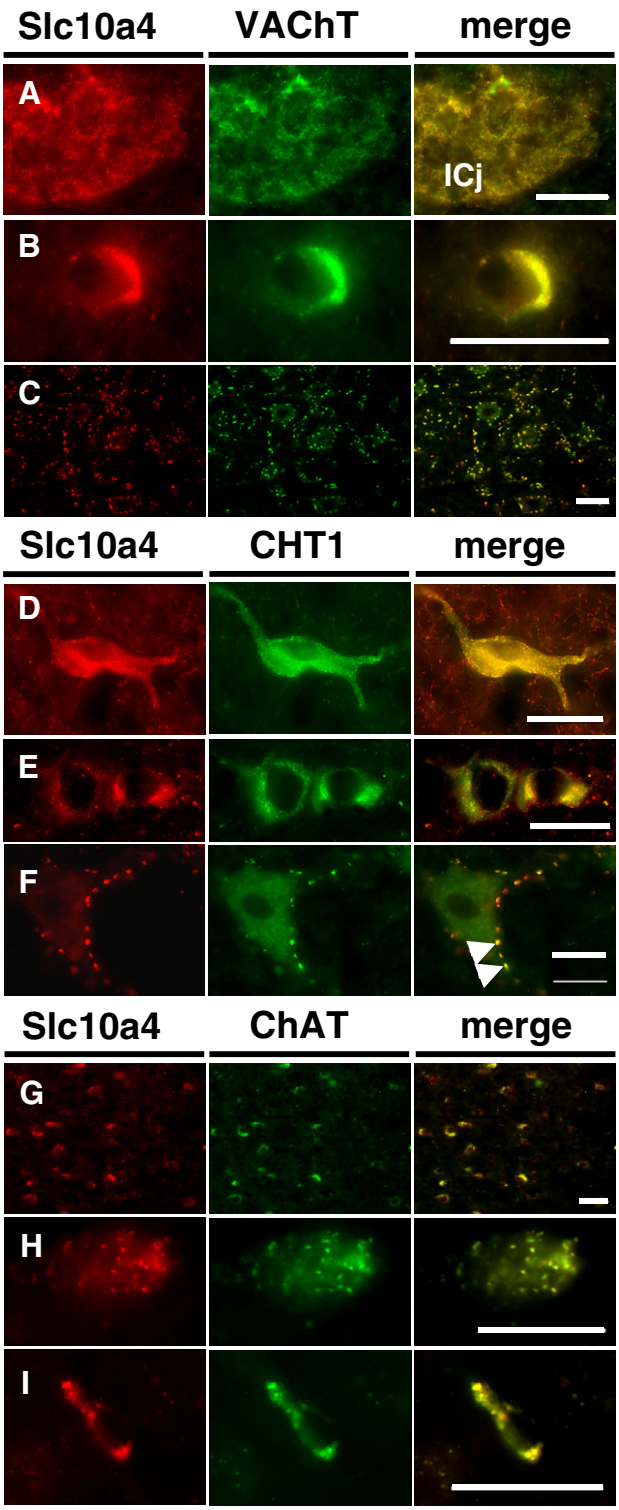

Fig. 6. Co-localization of Slc10a4 expression with VAChT, CHT1, and ChAT. Coronal sections of the rat CNS were analyzed for Slc10a4 (A–I), VAChT (A–C), CHT1 (D–F), and ChAT (G–I) immunoreactivities. Merged images are shown to illustrate co-localization between Slc10a4 and VAChT (A–C), Slc10a4 and CHT1 (D–F), and Slc10a4 and ChAT (G–I). (A) Dense staining of Slc10a4-immunopositive and VAChT-immunopositive fibers and puncta was observed in the island of Calleja. (B) Slc10a4 and VAChT co-expression was found in cell bodies of the accumbens nucleus. (C) In the ventral horn of the spinal cord, Slc10a4-immunoreactivity and VAChT-immunoreactivity are present in cell bodies of motor neurons as well as in the large presynaptic C-boutons that surround them. (D) Intense Slc10a4-like and CHT1-like immunoreactivities are detected in neuronal cell bodies of the olfactory tubercle. (E) Slc10a4-immunopositive and CHT1-immunopositive cell bodies are observed in the nucleus of the horizontal limb of the diagonal band. (F) Co-expression of Slc10a4 and CHT1 occurs in the motor trigeminal nuclei; nerve terminals are indicated by arrows. (G, H) Staining of Slc10a4-immunopositive and ChAT-immunopositive cell bodies was seen in the ventral tegmental area; immunoreactivity was concentrated in intracellular vesicular compartments. (I) Slc10a4 and ChAT co-expression in neuronal cell bodies was observed in the SN. Scale bars=50 μm (A, C, G); 25 μm (B, D–F, H, I).

When we used this Slc10a4 antiserum for Western blot analysis of various regions of the rat CNS, a second band at ~73 kDa was found in almost all brain regions, in addition to the ~47 kDa band that most likely represents the native form of the protein. As the Slc10a4 protein sequence contains five potential outer-facing N-glycosylation sites (Asn^{6}, Asn^{20}, Asn^{26}, Asn^{181}, and Asn^{195}) that are conserved among the rat Slc10a4 protein and the human SLC10A4 protein, this band of higher molecular weight probably represent the mature glycosylated form of the Slc10a4 protein. This was already assumed for the human SLC10A4 protein by Splinter and coworkers (2006), who did Western blot analysis of CHO cells stably transfected with a V5-epitope tagged human SLC10A4 protein and found a larger band of ~80 kDa in addition to a smaller ~49 kDa band. In our transiently Slc10a4-FLAG/Slc10a4 transfected HEK293 cells by contrast, only a single dominant band at ~48 kDa/~47 kDa occurred, indicating that only the native non-glycosylated Slc10a4 protein is expressed in the HEK293 cells under these experimental conditions.

In general, Slc10a4-specific immunofluorescence staining clearly merged with VAChT-specific and CHT1-specific immunoreactivities, but in a few specific regions, the expression of the Slc10a4 protein was apparently higher (basolateral amygdaloid nucleus, ventral tegmental area, SN, and dorsal motor nucleus of vagus) or lower (nucleus of the vertical limb of the diagonal band, medial septal nucleus, caudate putamen, and basal nucleus of Meynert) than the expression of VAChT and CHT1. Predominant staining of Slc10a4-positive neuronal cell bodies and fibers was particularly detected by immunohistochemistry in the SN. Data from the Allen Brain Atlas also show strong hybridization signals for the mouse Slc10a4 transcript in the SN (Lein et al., 2007) pointing to a particular importance of Slc10a4 in this brain region. As expected from earlier studies (Gilmor et al., 1996; Okuda et al., 2000; Misawa et al., 2001), immunostaining for VAChT and CHT1 was not observed in the SN. In contrast, expression of ChAT was detected in neurons of the SN, and this enzyme showed an expression pattern very similar to that of Slc10a4, namely at the transition zone between the SN compact and reticular compartment (Martinez-Murillo et al., 1989). As shown in Fig. 6, we found co-localization of Slc10a4-specific and ChAT-specific immu-

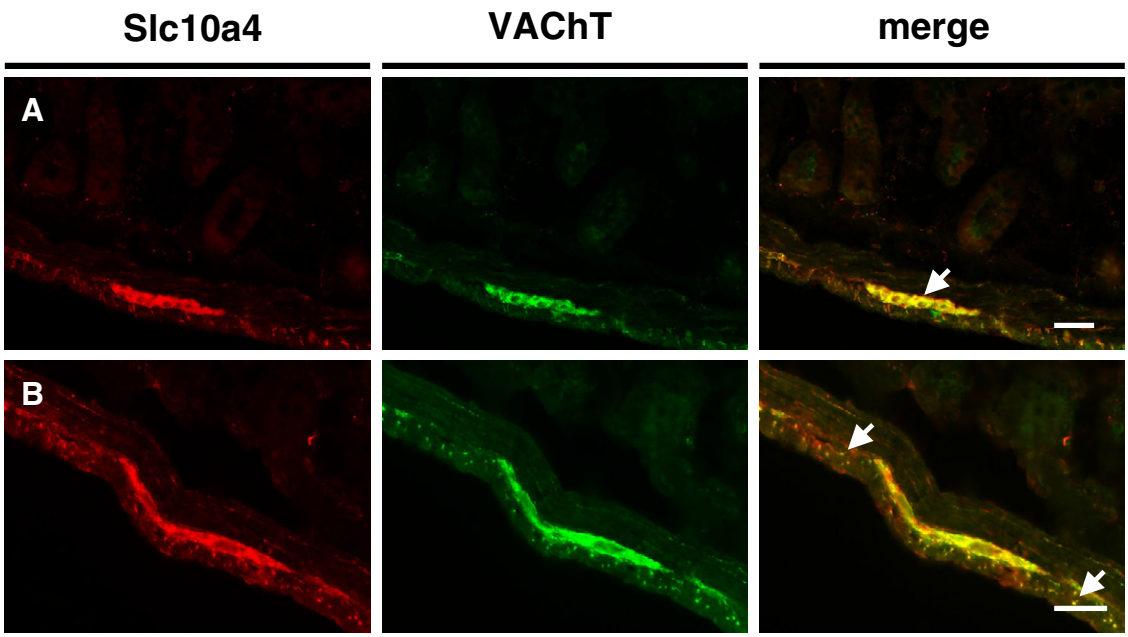

Fig. 7. Co-localization of Slc10a4 expression with VAChT in the enteric nervous system. Sections of various intestinal regions were analyzed for Slc10a4 and VAChT immunoreactivities. Merged images are shown to indicate co-localization of both proteins. (A) Dense staining of Slc10a4- and VAChT-immunopositive neuronal cell bodies in the myenteric plexus (indicated by arrow) of the terminal ileum. (B) Slc10a4 and VAChT co-expression was found in cell bodies as well as fibers (indicated by arrows) lining the myenteric plexus in the proximal duodenum. Scale bar=50 μm.

noreactivities in neuronal cell bodies of the SN, confirming that Slc10a4 is expressed in cholinergic neurons also in this brain region. In a recent study, Jørgensen and coworkers (2006) found significant up-regulation of SLC10A4 mRNA expression during the development of the human ventral mesencephalon. They stated that SLC10A4 might be a candidate marker gene for dopaminergic progenitor neurons. Although it cannot be ruled out that Slc10a4 expression in the SN occurs also in dopaminergic neurons, this would not concur with the general expression pattern in cholinergic neurons of the rat brain shown by VAChT, CHT1, and ChAT co-labeling studies.

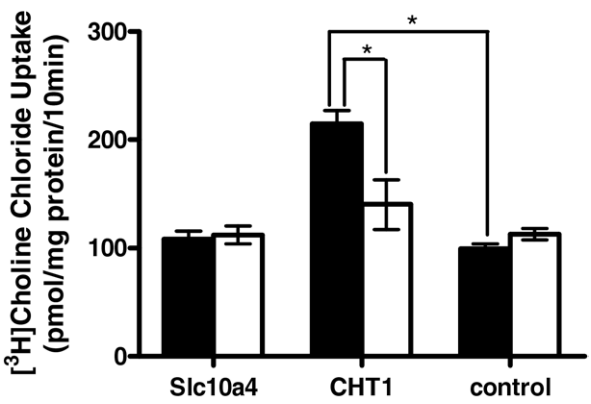

Fig. 8. Transport experiments with choline in HEK293 cells transfected with rat Slc10a4 and rat CHT1. The uptake of [^{3}H]choline chloride (1 μM) was measured over a time period of 10 min in the presence (open bars) and absence (filled bars) of 1 μM hemicholinium-3 as inhibitor at 37 °C. The cells were washed with ice-cold PBS, lysed, and subjected to scintillation counting. The values represent means±S.D. of a representative experiment with quadruplicate determinations. * Statistically different uptake ($P<0.01$).

The gene expression patterns of human SLC10A4 and rat Slc10a4 are not identical. Whereas rat Slc10a4 is predominantly expressed in the brain (Fig. 2A), human SLC10A4 has been claimed to be ubiquitously expressed in human tissues, as high amounts of SLC10A4 mRNA were detected in brain, placenta, and pancreas and lower levels in liver, kidney, and organs of the digestive system by Northern blot analysis (Splinter et al., 2006). The expression of SLC10A4 in the pancreas is doubtful though, because a highly truncated 0.7 kb mRNA transcript was detected in this study that would not express the full-length SLC10A4 protein of 437 amino acids. In contrast to that previous report, we found higher expression of human SLC10A4 mRNA in the gut than in the placenta (Fig. 2). We observed by immunohistochemistry that expression of the rat Slc10a4 protein in the gut occurs in cholinergic neurons of the enteric nervous system but not in enterocytes, where the intestinal bile acid carrier Asbt (Slc10a2) was localized (Shneider et al., 1995). So our results demonstrate a specialized expression in the peripheral nervous system but cannot be interpreted as a ubiquitous organ expression pattern of SLC10A4/Slc10a4.

A significant gap in the research on SLC10A4/Slc10a4 is the lack of information on the substrate pattern of this carrier protein. Neither the human SLC10A4 (Splinter et al., 2006) nor the rat Slc10a4 protein (Table 1) showed transport activity for taurocholate. The sulfoconjugated neurosteroids DHEAS and PREGS, which are substrates of Ntcp and Soat, were prime candidate transportates of Slc10a4. These steroids are present in the CNS at high

concentrations and exert multiple effects on neuronal excitability, neuronal plasticity, and neuroprotection (Baulieu, 1998; Rupprecht and Holsboer, 1999; Wolf and Kirschbaum, 1999; Schumacher et al., 2000; Mellon and Griffin, 2002; Dubrovsky, 2005). But none of these neurosteroids was transported by Slc10a4, as shown by transport experiments in *Xenopus laevis* oocytes and HEK293 cells expressing the rat Slc10a4 protein. So far, we have also not been able to unravel a particular transport function in cholinergic neurons with choline chloride as another possible candidate substrate (Fig. 8).

CONCLUSION

In conclusion, contradictory to previous suggestions about a ubiquitous function of the SLC10A4 protein in the cell machinery by Splinter and coworkers (2006), we find that in man, rat, and mouse, SLC10A4/Slc10a4 mRNA is most highly expressed in the brain and that the rat Slc10a4 protein is distinctively expressed in cholinergic neurons, at least in the CNS and gut. Therefore, we assume a highly specialized neuronal function for the Slc10a4 protein that requires further investigation.

Acknowledgments—The authors wish to acknowledge Klaus Schuh and Doreen Marks for technical help. The authors would like to thank Michael Hanna, PhD (Medical Manuscript Service, New York) for proofreading the manuscript. This study was supported by the Brazilian-German CAPES/DAAD exchange program (C.F.F.), and the German Research Foundation (DFG), Graduate Research Program 455 "Molecular Veterinary Medicine" (B.D. and J.R.G.). The nucleotide sequence reported in this article has been deposited under GenBank accession number AY825923.

REFERENCES

Alrefai WA, Gill RK (2007) Bile acid transporters: structure, function, regulation and pathophysiological implications. Pharm Res 24: 1803–1823.

Ananthanarayanan M, Ng OC, Boyer JL, Suchy FJ (1994) Characterization of cloned rat liver Na(+)-bile acid cotransporter using peptide and fusion protein antibodies. Am J Physiol 267:G637–G643.

Apparsundaram S, Ferguson SM, George AL Jr, Blakely RD (2000) Molecular cloning of a human, hemicholinium-3-sensitive choline transporter. Biochem Biophys Res Commun 276:862–867.

Armstrong DM, Saper CB, Levey AI, Wainer BH, Terry RD (1983) Distribution of cholinergic neurons in rat brain: demonstrated by the immunocytochemical localization of choline acetyltransferase. J Comp Neurol 216:53–68.

Baulieu EE (1998) Neurosteroids: a novel function of the brain. Psychoneuroendocrinology 23:963–987.

Chen NH, Reith ME, Quick MW (2004) Synaptic uptake and beyond: the sodium- and chloride-dependent neurotransmitter transporter family SLC6. Pflügers Arch 447:519–531.

Colman A (1984) Translation of eukaryotic messenger RNA in *Xenopus* oocytes. In: Transcription and translation. A practical approach (Hames BD, Higgins SJ, eds), pp 271–302. Oxford: IRL Press Limited.

Dubrovsky BO (2005) Steroids, neuroactive steroids and neurosteroids in psychopathology. Prog Neuropsychopharmacol Biol Psychiatry 29:169–192.

Eckenstein F, Thoenen H (1982) Production of specific antisera and monoclonal antibodies to choline acetyltransferase: Characterization and use for identification of cholinergic neurons. EMBO J 1: 363–368.

Ferguson SM, Savchenko V, Apparsundaram S, Zwick M, Wright J, Heilman CJ, Yi H, Levey AI, Blakely RD (2003) Vesicular localization and activity-dependent trafficking of presynaptic choline transporters. J Neurosci 23:9697–9709.

Fernandes CF, Godoy JR, Döring B, Cavalcanti MCO, Bergmann M, Petzinger E, Geyer J (2007) The novel putative bile acid transporter SLC10A5 is highly expressed in liver and kidney. Biochem Biophys Res Commun 361:26–32.

Gether U, Andersen PH, Larsson OM, Schousboe A (2006) Neurotransmitter transporters: molecular function of important drug targets. Trends Pharmacol Sci 27:375–383.

Geyer J, Godoy JR, Petzinger E (2004a) Identification of a sodium-dependent organic anion transporter from rat adrenal gland. Biochem Biophys Res Commun 316:300–306.

Geyer J, Döring B, Failing K, Petzinger E (2004b) Molecular cloning and functional characterization of the bovine (*Bos taurus*) organic anion transporting polypeptide Oatp1a2 (Slco1a2). Comp Biochem Physiol B Biochem Mol Biol 137:317–329.

Geyer J, Wilke T, Petzinger E (2006) The solute carrier family SLC10: more than a family of bile acid transporters regarding function and phylogenetic relationships. Naunyn Schmiedebergs Arch Pharmacol 372:413–431.

Geyer J, Döring B, Meerkamp K, Ugele B, Bakhiya N, Fernandes CF, Godoy JR, Glatt H, Petzinger E (2007) Cloning and functional characterization of human sodium-dependent organic anion transporter (SLC10A6). J Biol Chem 282:19728–19741.

Gilmor ML, Nash NR, Roghani A, Edwards RH, Yi H, Hersch SM, Levey AI (1996) Expression of the putative vesicular acetylcholine transporter in rat brain and localization in cholinergic synaptic vesicles. J Neurosci 16:2179–2190.

Godoy JR, Fernandes C, Döring B, Beuerlein K, Petzinger E, Geyer J (2007) Molecular and phylogenetic characterization of a novel putative membrane transporter (SLC10A7), conserved in vertebrates and bacteria. Eur J Cell Biol 86:445–460.

Hagenbuch B, Lubbert H, Stieger B, Meier PJ (1990) Expression of the hepatocyte Na^+/bile acid cotransporter in *Xenopus laevis* oocytes. J Biol Chem 265:5357–5360.

Hagenbuch B, Stieger B, Foguet M, Lubbert H, Meier PJ (1991) Functional expression cloning and characterization of the hepatocyte Na^+/bile acid cotransport system. Proc Natl Acad Sci U S A 88:10629–10633.

Hagenbuch B, Dawson P (2004) The sodium bile salt cotransport family SLC10. Pflügers Arch 447:566–570.

Hediger MA, Romero MF, Peng JB, Rolfs A, Takanaga H, Bruford EA (2004) The ABCs of solute carriers: physiological, pathological and therapeutic implications of human membrane transport proteins. Introduction. Pflügers Arch 447:465–468.

Jørgensen JR, Juliusson B, Henriksen KF, Hansen C, Knudsen S, Petersen TN, Blom N, Seiger A, Wahlberg LU (2006) Identification of novel genes regulated in the developing human ventral mesencephalon. Exp Neurol 198:427–437.

Kanai Y, Hediger MA (2003) The glutamate and neutral amino acid transporter family: physiological and pharmacological implications. Eur J Pharmacol 479:237–247.

Kus L, Borys E, Ping CY, Ferguson SM, Blakely RD, Emborg ME, Kordower JH, Levey AI, Mufson EJ (2003) Distribution of high affinity choline transporter immunoreactivity in the primate central nervous system. J Comp Neurol 463:341–357.

Lein ES, Hawrylycz MJ, et al. (2007) Genome-wide atlas of gene expression in the adult mouse brain. Nature 445:168–176.

Levey AI, Armstrong DM, Atweh SF, Terry RD, Wainer BH (1983a) Monoclonal antibodies to choline acetyltransferase: production, specificity, and immunohistochemistry. J Neurosci 3:1–9.

Levey AI, Wainer BH, Mufson EJ, Mesulam MM (1983b) Co-localization of acetylcholinesterase and choline acetyltransferase in the rat cerebrum. Neuroscience 9:9–22.

Lowry OH, Rosebrough NJ, Farr AL, Randall RJ (1951) Protein measurement with the folin phenol reagent. J Biol Chem 193:265–275.

Martinez-Murillo R, Villalba R, Montero-Caballero MI, Rodrigo J (1989) Cholinergic somata and terminals in the rat substantia nigra: an immunocytochemical study with optical and electron microscopic techniques. J Comp Neurol 281:397–415.

Masson J, Sagne C, Hamon M, El Mestikawy S (1999) Neurotransmitter transporters in the central nervous system. Pharmacol Rev 51:439–464.

Meier PJ, Stieger B (2002) Bile salt transporters. Annu Rev Physiol 64:635–661.

Mellon SH, Griffin LD (2002) Neurosteroids: biochemistry and clinical significance. Trends Endocrinol Metab 13:35–43.

Misawa H, Nakata K, Matsuura J, Nagao M, Okuda T, Haga T (2001) Distribution of the high-affinity choline transporter in the central nervous system of the rat. Neuroscience 105:87–98.

Okuda T, Haga T, Kanai Y, Endou H, Ishihara T, Katsura I (2000) Identification and characterization of the high-affinity choline transporter. Nat Neurosci 3:120–125.

Okuda T, Haga T (2000) Functional characterization of the human high-affinity choline transporter. FEBS Lett 484:92–97.

Paxinos G, Watson C (2004) The rat brain in stereotaxic coordinates, fifth edition. San Diego: Elsevier Academic Press.

Ribeiro FM, Alves-Silva J, Volknandt W, Martins-Silva C, Mahmud H, Wilhelm A, Gomez MV, Rylett RJ, Ferguson SS, Prado VF, Prado MA (2003) The hemicholinium-3 sensitive high affinity choline transporter is internalized by clathrin-mediated endocytosis and is present in endosomes and synaptic vesicles. J Neurochem 87:136–146.

Rupprecht R, Holsboer F (1999) Neuroactive steroids: mechanisms of action and neuropsychopharmacological perspectives. Trends Neurosci 22:410–416.

Schumacher M, Akwa Y, Guennoun R, Robert F, Labombarda F, Desarnaud F, Robel P, De Nicola AF, Baulieu EE (2000) Steroid synthesis and metabolism in the nervous system: trophic and protective effects. J Neurocytol 29:307–326.

Shneider BL, Dawson PA, Christie DM, Hardikar W, Wong MH, Suchy FJ (1995) Cloning and molecular characterization of the ontogeny of a rat ileal sodium-dependent bile acid transporter. J Clin Invest 95:745–754.

Splinter PL, Lazaridis KN, Dawson PA, LaRusso NF (2006) Cloning and expression of SLC10A4, a putative organic anion transport protein. World J Gastroenterol 12:6797–6805.

Stieger B, Hagenbuch B, Landmann L, Hochli M, Schroeder A, Meier PJ (1994) In situ localization of the hepatocytic Na^+/taurocholate cotransporting polypeptide in rat liver. Gastroenterology 107:1781–1787.

Trauner M, Boyer JL (2003) Bile salt transporters: molecular characterization, function, and regulation. Physiol Rev 83:633–671.

Weihe E, Tao-Cheng JH, Schafer MK, Erickson JD, Eiden LE (1996) Visualization of the vesicular acetylcholine transporter in cholinergic nerve terminals and its targeting to a specific population of small synaptic vesicles. Proc Natl Acad Sci U S A 93:3547–3552.

Wolf OT, Kirschbaum C (1999) Actions of dehydroepiandrosterone and its sulfate in the central nervous system: effects on cognition and emotion in animals and humans. Brain Res Brain Res Rev 30:264–288.

Wong MH, Oelkers P, Craddock AL, Dawson PA (1994) Expression cloning and characterization of the hamster ileal sodium-dependent bile acid transporter. J Biol Chem 269:1340–1347.

(Accepted 4 February 2008)
(Available online 8 February 2008)